Neuron, Vol. 25, 459–471, February, 2000, Copyright ©2000 by Cell Press

Diversity and Cell Type Specificity of Local Excitatory Connections to Neurons in Layer 3B of Monkey Primary Visual Cortex

Atomu Sawatari and Edward M. Callaway*
Systems Neurobiology Laboratories
The Salk Institute for Biological Studies
La Jolla, California 92037

Summary

In the primary visual cortex of macaque monkeys, laminar and columnar axonal specificity are correlated with functional differences between locations. We describe evidence that embedded within this anatomical framework is finer specificity of functional connections. Photostimulation-based mapping of functional input to 31 layer 3B neurons revealed that input sources to individual cells were highly diverse. Although some input differences were correlated with neuronal anatomy, no 2 neurons received excitatory input from the same cortical layers. Thus, input diversity reveals far more cell types than does anatomical diversity. This implies relatively little functional redundancy; despite trends related to laminar or columnar position, pools of neurons contributing uniquely to visual processing are likely relatively small. These results also imply that similarities in the anatomy of circuits in different cortical areas or species may not indicate similar functional connectivity.

Introduction

A major aim of systems neurobiology research is to understand how neural circuits give rise to cortical function. Present understanding of cortical circuits is based primarily on anatomical observations revealing specific projection patterns of axonal arbors and the spatial overlap of these axons with the dendritic arbors of other neurons. When axons and dendrites overlap, there are, potentially, connections. This approach has been used to reveal anatomical relationships between neural circuits and functional subdivisions (e.g., cortical layers and columns) in the primary visual cortex (V1) of macaque monkeys (Livingstone and Hubel, 1984b; Lachica et al., 1992; Yoshioka et al., 1994; Callaway and Wiser, 1996; Wiser and Callaway, 1996; Yabuta and Callaway, 1998a, 1998b; see Callaway, 1998, for review). These correlations are the basis of inferences about how neural circuits mediate cortical function.

It is apparent, however, that neural circuits have the potential to be far more complex than suggested by anatomical observations. For example, Stevens (1998) has suggested, based on theoretical "tiling" arguments, that there may be hundreds of distinct cell types in each cortical layer. This is far more than suggested by the anatomical diversity of cortical neurons. Although extreme diversity of neuron types has been revealed in the retina by morphological criteria (MacNeil and Masland, 1998), it need not be the case that connectional differences correspond one-to-one to morphological differences. In the hippocampus, greater diversity of inhibitory neurons is revealed by physiological measures than by anatomy alone (Parra et al., 1998). We show here that diversity can also arise from differential input to anatomically indistinguishable cell types.

Macaque V1 offers several advantages for addressing these issues. Primate V1 contains numerous laminar and columnar subdivisions that segregate the area into functionally distinct regions (see Callaway, 1998, for review), and intracellular labeling and Golgi studies have extensively documented the morphological neuron types in V1 (Lund, 1987; Lund et al., 1988; Katz et al., 1989; Lund and Yoshioka, 1991; Anderson et al., 1993; Callaway and Wiser, 1996; Wiser and Callaway, 1996; Yabuta and Callaway, 1998b). Thus, macaque V1 serves as a useful model system in which it is not only possible to investigate relationships between cortical circuits and visual function but also between anatomy and functional connectivity.

Here, we describe investigations of functional connectivity revealed by laser scanning photostimulation (Callaway and Katz, 1993; Dalva and Katz, 1994; Katz and Dalva, 1994; Sawatari and Callaway, 1996). With this method, we have studied the sources of functional excitatory input to individual layer 3B neurons in living brain slices from macaque V1. We focused on layer 3B because it receives anatomical input from excitatory neurons in each of the 7 deeper cortical layers (layers 4A, 4B, 4Cα, 4Cm, 4Cβ, 5, and 6), yet individual neurons are highly diverse in their responses to visual stimuli (Hubel and Wiesel, 1968, 1974; Livingstone and Hubel, 1984a; Ts'o et al., 1986; Tootell et al., 1988a, 1988b, 1988c; Edwards et al., 1995). It is unknown whether the anatomical organization implies that every layer 3B neuron receives functional connections from all the deeper layers, or whether each deep layer afferent might selectively connect onto a subset of the layer 3B neurons whose dendrites overlap with their axonal arbors. Increased selectivity of functional connections relative to anatomical axonal arborization could account for the functional diversity of layer 3B neurons and would provide novel insight into general rules about cortical connectivity.

We found that the sources of functional excitatory input to individual layer 3B neurons were extremely diverse. No 2 cells from our population of 31 neurons received detectable input from the same combination of layers. Twenty-seven of these neurons were pyramidal cells that could be divided into two morphologically distinct groups, local pyramids and projecting pyramids. Functional connections were detected from layer 4Cβ onto most local pyramids but never onto projecting pyramids, despite dense anatomical input from layer 4Cβ to layer 3B (cf. Yabuta and Callaway, 1998b). Thus, there was a systematic difference in input to these 2 cell types, but even within these groups, the precise sources of laminar input were highly diverse. Finally, we detected

*To whom correspondence should be addressed (e-mail: callaway@salk.edu).

differences in the sources of excitatory input to layer 3B neurons in cytochrome-oxidase (CO) blobs versus interblobs, consistent with anatomical differences in blob and interblob projections, but these differences were not as pronounced as suggested by the anatomy.

Results

Overview

Sources of local excitatory input to 31 layer 3B neurons were measured in macaque V1 brain slices (27 pyramidal cells, 3 inhibitory cells, and 1 cell of unknown morphology) using scanning laser photostimulation. Photostimulation combines standard whole-cell recording in living brain slices with the light-induced release of "caged" glutamate to reveal sources of excitatory input to individual neurons (Dalva and Katz, 1994; Katz and Dalva, 1994; Sawatari and Callaway, 1996). Only neurons with cell bodies very near the uncaging site generate action potentials (APs) (see Experimental Procedures). Thus, if inward excitatory postsynaptic currents (EPSCs) are evoked by photostimulation, it can be inferred that a neuron(s) with its cell body(ies) near the stimulation site made monosynaptic excitatory connections onto the recorded cell (see Experimental Procedures). Since photostimulation is noninvasive, and the location of uncaging can be readily moved, hundreds of sites within the slice can be stimulated. Thus, a "map" of the locations of neurons providing excitatory input to the recorded cell can be generated.

To exemplify the collection and analysis of photostimulation data, Figure 1 illustrates the results obtained from 2 layer 3B pyramidal neurons. For each cell, camera lucida reconstructions were made of both the labeled neuron and the laminar borders. The colored squares in the figure indicate the locations of stimulation sites (additional overlapping sites omitted for clarity). Laser-marked "alignment sites" (data not shown) were used to align the stimulation sites with the anatomical reconstructions (see Experimental Procedures). The colors of the squares indicate either the number (Figures 1A and 1C) or the sum of peak amplitudes (Figures 1B and 1D) of EPSCs measured following stimulation at that site. The panels flanking the anatomical reconstructions depict whole-cell voltage-clamp recordings (-65 mV holding potential) measured following stimulation at the sites indicated by the arrows. For example, the top right panel in Figure 1B shows EPSCs recorded following photostimulation in layer 4B. Two EPSCs were detected at this stimulation site, with the sum of their amplitudes equaling $\sim$40 pA. Figure 1 also illustrates typical columnar distributions of stimulation sites. Stimulation was restricted to within 500 μm (usually $<$300 μm) laterally from the vertical column containing the cell body. This was done because anatomical observations have shown that interlaminar connections are formed predominantly by vertically projecting axons (cf. Lachica et al., 1992; Yoshioka et al., 1994; Callaway and Wiser, 1996; Wiser and Callaway, 1996; Yabuta and Callaway, 1998b). The possibility that axons providing input to a neuron are cut during slice preparation is therefore minimized for cells in nearby columns.

The responses illustrated in Figure 1 do not directly reveal the sources of excitatory input to each cell. This is because during whole-cell recording, spontaneous EPSCs (sEPSCs) were commonly observed. In layer 3B neurons, sEPSCs were detected at frequencies, on average, of 2.8 Hz. Since responses generated within a 150 ms time window after photostimulation were considered for our analyses (see Experimental Procedures), the rate of spontaneous current production translated into a mean of 0.42 sEPSCs per 150 ms analysis window. Thus, responses measured following photostimulation were a combination of spontaneous currents and stimulus-evoked EPSCs. Further analysis was therefore required to reveal whether stimulation within a given region (e.g., cortical layer) did in fact result in the generation of evoked EPSCs.

To determine whether a given layer provided excitatory input to a cell, EPSCs measured after photostimulation in that layer were compared statistically with spontaneous currents measured in the absence of stimuli for the same neuron (see Experimental Procedures). These comparisons were made for each of three measures of EPSCs occurring within the 150 ms analysis window: number, peak amplitude, and the sum of peak amplitudes. Only those layers in which EPSCs were statistically different from controls ($p \leq 0.05$; see Experimental Procedures for details) were considered to provide significant input. To determine the relative input from each layer to a given cell, histograms were generated depicting an estimate of the mean number of evoked EPSCs per stimulation site (estimated mean evoked $=$ mean photostimulation $-$ mean spontaneous) obtained for each layer (e.g., see Figure 6).

Finally, in order to examine possible differences in excitatory laminar input between populations of cells, neurons in our sample were first grouped by either their morphological features or by the location of their cell bodies with respect to CO blobs. Statistical comparisons were then conducted between these populations (Fisher's exact test) to determine whether there were differences in the proportion of cells receiving statistically significant input from each layer.

Overall Results

Figure 2 illustrates the proportions of the 31 neurons in our sample that received statistically significant input (number, peak amplitude, or sum of peak amplitudes of EPSCs) from each of the cortical layers. These data, pooled from the entire population, show that each of the cortical layers provided statistically significant input to some layer 3B neurons. This result is expected from anatomical observations showing that every layer in macaque V1 contains excitatory neurons with axonal arbors in layer 3B (see Callaway 1998, for review). (Figure 2 should not be interpreted as an indication of the relative strength of connections to layer 3B from the various layers. This is because the ability to detect significant input from a layer is dependent on the number of stimulation sites in a layer, and thinner layers (e.g., 4Cm) tended to have fewer sites.) Anatomical observation cannot, however, reveal whether every cell receives input from each layer or whether the organization of connections

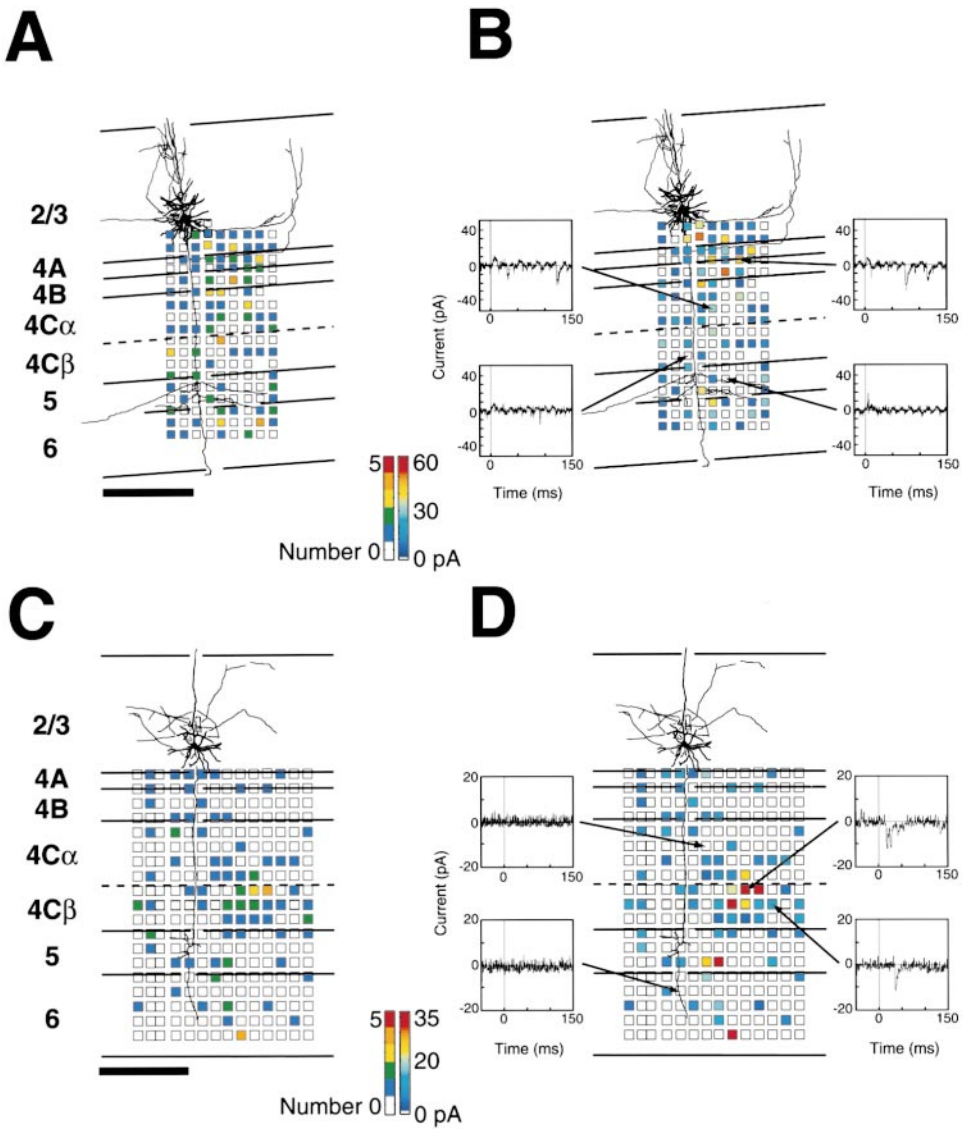

Figure 1. Photostimulation-Based Maps of Excitatory Input to Layer 3B Pyramidal Neurons

The maps illustrate the numbers (A and C) and sums of peak amplitudes (B and D) of EPSCs measured from a layer 3B projecting pyramid (A and B) and a local pyramid (C and D) superimposed on their respective camera lucida reconstructions (dendrites, thick lines; axons, thinner lines). Each colored square corresponds to a photostimulation site. Although each site was stimulated multiple times during the course of the experiments, for clarity, spatially overlapping sites are omitted. The colors indicate, according to the scale bars, the number (A and C) or sum of peak amplitudes (in pA; B and D) of EPSCs measured following stimulation at that site. The sites with no detectable responses have white squares. Representative whole-cell voltage-clamp recordings measured immediately before and for 150 ms after photostimulation are shown in (B) and (D). Arrows point to the stimulation sites corresponding to each recording. For the projecting pyramid, EPSCs significantly greater than expected from sEPSCs, both in number and sum of peak amplitudes, were detected following photostimulation in layers 3B, 4A, and 4Cα. In addition, EPSC amplitudes (but not sum or number) were significantly greater than for sEPSCs following stimulation in layer 4B (see Table 1, cell b35c11). This pattern of input contrasts with the sources of significant input to the local pyramid. For the local pyramid, EPSC number was significantly increased only by photostimulation in layer 4Cβ. Boundaries between layers are represented by horizontal lines. The names of the layers are shown to the left of (A) and (C). Scale bar, (thick black lines), 300 μm (A and C).

is more precise. Indeed, individual cells typically had more restricted and highly specific laminar input (Table 1). The sources of input were dependent on whether or not the cell's axon projected to the white matter and on the location of the cell's soma relative to CO blobs. However, even among neurons that fell into a single group based on these criteria, sources of input were diverse.

Projecting versus Local Pyramidal Neurons

Most layer 3B pyramidal cells in macaque V1 are "local" excitatory neurons that lack axonal projections out of V1 (Rockland and Pandya, 1979; Yukie and Iwai, 1985; Callaway and Wiser, 1996; see also below). In our sample, 7 of 27 pyramidal neurons were identified as projecting pyramids. Cells were considered projecting if their main descending axon extended into the white

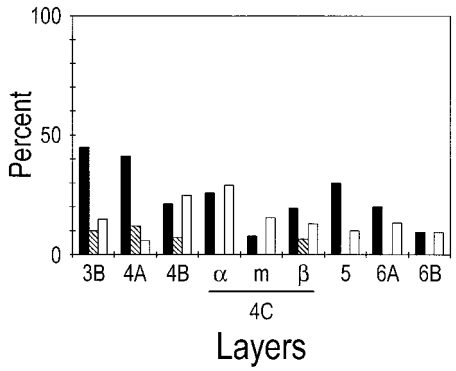

Figure 2. Percentages of Layer 3B Neurons Receiving Significant Input from Each Cortical Layer

The histogram depicts the percentages of layer 3B neurons that received significant input, based on EPSC number, sum of peak amplitudes, or individual peak amplitudes from each of the underlying layers. Closed bars correspond to significant increases in EPSC number following stimulation in the relevant layer. Hatched bars correspond to significant increases in the sums of EPSC amplitudes but not number. Open bars correspond to significant increases in amplitudes of individual EPSCs but not number or sums of amplitudes. Overall, statistically significant input was detected to this population of layer 3B neurons from all layers. But, typically only about 30%–60% of the cells received significant input from any given layer.

matter. Nonprojecting neurons ("local pyramids," 13 of 27) were identified as cells whose descending axons clearly ended above the white matter without leaving the plane of the brain slice. For the pyramidal neurons, 7 of 27 were classified as ambiguous because their descending axons left the plane of the brain slice, making definitive characterization impossible. If ambiguous neurons are excluded, the percentages of projecting and nonprojecting pyramids were 35% (7 of 20) and 65% (13 of 20), respectively.

Figure 3 shows two examples each of projecting and local pyramids. The 2 projecting neurons (Figure 3A) had apical dendritic tufts (see arrows in Figure 3A), while the 2 local pyramids (Figure 3B) did not. All 7 of the projecting pyramids in our sample had tufted apical dendrites. Of the 13 pyramidal neurons that were confirmed to have their axons terminating before reaching the white matter, only 2 had apical dendritic tufts. Projections to the white matter were not observed for any of 18 nontufted neurons (11 nonprojecting, 7 ambiguous). The difference in the proportions of tufted cells that projected or did not project to the white matter was statistically significant (Fisher's exact test, $p = 0.00046$).

We found that these anatomical features, particularly axonal projections, were correlated with sources of excitatory input identified by photostimulation. The most striking difference was that significant input from the parvocellular dorsal lateral geniculate nucleus (dLGN) recipient layer, 4Cβ, was restricted to only the local pyramids in our sample. As illustrated in Figure 4A, none of the 7 projecting pyramids received statistically significant input from this layer. In contrast, 8 of the 13 local pyramids (62%) received statistically significant input from layer 4Cβ. The difference between the two groups was significant (Fisher's exact test, $p = 0.010$).

A difference was also detected in input from layer 4B to local versus projecting pyramids (Figure 4A). Although there was not a significant difference in the proportion of cells receiving significant layer 4B input when all EPSC parameters (number, individual amplitudes, amplitude sums) were considered, there was a bias toward projecting pyramids. But, significant increases in individual EPSC peak amplitudes following layer 4B stimulation relative to control trials were much more common for projecting pyramids than for local pyramids. A significant increase in EPSC peak amplitudes was detected for 5 of 7 (71%) projecting pyramids compared with only 1 of 12 (8%) local pyramids (Fisher's exact test, $p = 0.009$).

These differences in input can be seen in the examples shown in Figure 1. For the local pyramid (Figures 1C and 1D), numerous EPSCs were observed following stimulation in layer 4Cβ (additional overlapping stimulation sites were omitted from the figure for clarity), and these were statistically more common than was the rate of sEPSCs. The mean number of EPSCs measured following stimulation within layer 4Cβ was 0.78 per stimulation site, while the rate of sEPSCs was 0.36 per "stimulation site." The difference between these distributions was statistically significant (Mann-Whitney U test, $p = 0.0072$). The estimated mean number of evoked EPSCs per stimulation site from each layer for this cell is illustrated in Figure 6F. For layer 4Cβ, this value was 0.43 evoked EPSCs per stimulation site. Only layer 4Cβ provided statistically significant input to this cell in terms of number of EPSCs. In contrast, for the projecting pyramid (Figures 1A and 1B), the number of EPSCs measured following stimulation in 4Cβ was not different from that of sEPSCs (see Table 1, cell b35c11). Instead, this cell received statistically significant input from layers 3B, 4A, 4B, and 4Cα.

Analysis of pyramidal neurons with ambiguous axonal projections also provided insight into differences in input to projecting versus local pyramids. All 7 of the ambiguous pyramids had apical dendrites that lacked tufts. Since none of the projecting pyramids in our sample lacked tufts, these cells were more likely to be local pyramids than projecting pyramids. We therefore pooled the local and ambiguous pyramids and compared them as a group with projecting pyramids (Figure 4B). Under these conditions, the differences in input from layers 4Cβ and 4B persisted (see Figure 4B legend).

Blobs versus Interblobs

Anatomical studies indicate that layer 3B CO blobs and interblobs receive specific axonal projections from underlying cortical layers (Lachica et al., 1992; Yoshioka et al., 1994; Callaway and Wiser, 1996; Yabuta and Callaway, 1998b). However, previous studies have also demonstrated that dendrites from both blob and interblob cells do not respect CO borders (Hubener and Bolz, 1992; Malach, 1992). It is therefore possible that the specific afferent projections from underlying cortical layers provide excitatory input onto dendrites of neurons with cell bodies outside the afferent projection zone.

To determine the specificity of laminar excitatory connections to individual neurons located in CO blobs and interblobs, cells were categorized as blob, border, or

Table 1. Tabulation of Laminar Input and Anatomical Characterization for All 31 Layer 3B Neurons

Cells	Morphology	CO Location	3B	4A	4B	4Cα	4Cm	4Cα+m	4Cβ	5	6A	6B
b32c10	T,P	B	a		a	a		a				
b38c2	T,P	B			n,s,a	a	None			n,s		
a40c3	T,P	B	n,s,a	n,s,a			NA				a	
b36c1	T,P	Bor	a	NA								
b32c2	T,P	lB	n,s,a	n,s	a		NA					None
b35c11	T,P	lB	n,s,a	n,s,a	a	n,s,a	NA	s,a				NA
b36c11	T,P	lB	NA	NA	a		NA			a		NA
b31c5	T,NP	B	None	NA	n,s	n,s	NA	n,s	n,s	n,s	n,s	n,s
b36c12	T,NP	B	n,s,a	n,s,a	n,s	n,s	NA	n,s	n,s	n,s	n,s	
b38c6	NT,NP	B	NA	NA	NA		NA			n,s		
a40c13	NT,NP	B	NA	a		a	None		n,s,a	a		
b38c1	NT,NP	Bor	n,s	n,s,a		n,s,a		n,s,a	n,s,a	n,s,a	n,s	n,s,a
b38c4	NT,NP	Bor	None	NA	n,s,a		NA		a			
a40c17	NT,NP	Bor	a			a	None			n,s,a	n,s,a	
b33c2	NT,NP	lB						a	s,a		a	NA
b34c6	NT,NP	lB		a			a	a	n,s,a	a		a
b35c2	NT,NP	lB	s,a	NA	s	n,s	n	n,s				NA
b36c2	NT,NP	lB	NA				NA		a			
a40c4	NT,NP	lB	n,s,a	n,s,a		n,s		n,s				
a40c5	NT,NP	?	s,a	n,s								
b34c4	NT,Amb	B		NA	a	a	NA	a			a	NA
b37c15	NT,Amb	B	NA	NA	NA	a	NA			NA	NA	NA
a40c16	NT,Amb	B	n,s	NA			NA	a				NA
b37c13	NT,Amb	Bor									a	
b38c12	NT,Amb	Bor	NA	NA	n,s				n,s	n,s		
b37c14	NT,Amb	lB	n,s	NA			NA				n,s	NA
a38c1	NT,Amb	lB	n,s		s,a	n,s	a	n,s	s,a	n,s	n,s	
b37c5	I	B	None	None	a	a		a	a	n,s,a		a
b35c5	I	Bor	NA	NA	n,s	n,s	NA	n,s	a			NA
b33c14	I	lB		s,a	a	a		a				
b37c3	U,U	Bor	NA	NA	NA	a	NA					

Each row represents data from a single neuron identified by cell number, type, and location. The first column identifies each cell by animal (e.g., b31) and cell number from that animal (e.g., c5). The second column identifies the morphological features of the cell's axonal and dendritic arbors. Abbreviations: T, tufted pyramid; NT, nontufted pyramid; I, inhibitory cell; P, projecting pyramid; NP, nonprojecting pyramid; Amb, ambiguous projection status; and U, unidentified. The third column indicates the location of the neuron's cell body relative to CO blobs. Abbreviations: B, blob; IB, interblob; Bor, border; and ?, undetermined. Columns 4–13 indicate whether layers 3B through 6B, respectively, provided significant excitatory input to each neuron: n = number of EPSCs per stimulation site were significantly greater than number of sEPSCs; s = sums of EPSC amplitudes per stimulation site were significantly larger than those of sEPSCs; a = individual peak amplitudes of EPSCs following photostimulation were significantly larger than those of sEPSCs; None = no sites were stimulated in the layer; and NA = fewer than ten sites were stimulated in the layer.

interblob neurons according to their cell body location. Statistical comparisons were then made to determine if there were differences in proportions of blob versus interblob neurons receiving significant input from each layer.

Our data revealed preferential connections from layers 4B, 4Cα, 4Cm, and 5 to cells in blobs or interblobs. But, these preferences depended on which attributes of EPSCs were used to detect significance of input to the individual neurons. When all three EPSC measures were taken into account (number, individual peak amplitudes, and sums of amplitudes), no layers exhibited a significant preference for blob or interblob cells. Preferences were revealed only when subsets of the three parameters were considered. The parameters that showed statistically significant input were different for different layers.

For layer 4B, a preference for connections to blob and border cells versus interblob cells was detected. But, the proportion of blob and border cells receiving significant input was only greater than that found for interblob cells if the statistical significance of input to each neuron was based solely on the number of EPSCs per stimulation site; cells with significant differences in EPSC amplitudes or sums of amplitudes (layer 4B stimulation trials versus control trials) but not number were discounted. Under these conditions, layer 4B provided significant excitatory input to 3 of 9 blob cells and 3 of 7 border cells but 0 of 11 interblob cells (Table 1). If blob and border cells were pooled together, 33% (6 of 16) received significant layer 4B input; compared with interblob neurons (0 of 11) the difference was statistically significant (Fisher's exact test, $p = 0.027$; see Figure 5B).

It is noteworthy, however, that when peak amplitudes and the sums of peak amplitudes were also included in the analysis, significant input from layer 4B was also detected for interblob neurons. When all three measures were included, 6 of 9 blob cells, 3 of 7 border cells, and 6 of 11 interblob cells received significant layer 4B input (Figure 5A). If the combination of blob and border cells was then compared with interblob neurons, the difference was no longer significant.

Based on EPSC amplitudes, layer 4Cα also made excitatory connections preferentially to blob cells. For

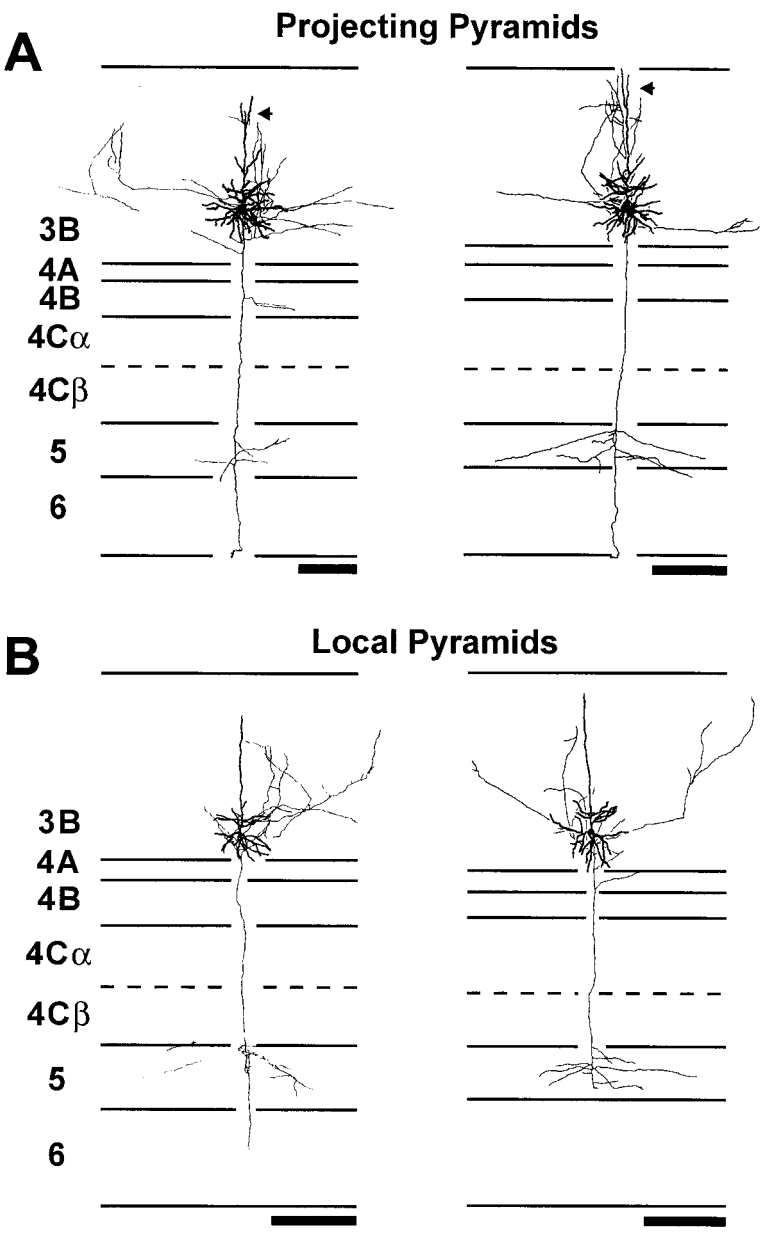

Figure 3. Camera Lucida Reconstructions of Layer 3B Projecting Pyramids and Local Pyramids

(A) Two projecting pyramidal neurons. The main descending axons extend into the white matter. Both of these projecting pyramids have tufts branching from the tops of their apical dendrites (arrows), as do all other projecting pyramids in our sample.

(B) Two local pyramidal neurons. The main descending axons of these neurons end within the plain of the parent brain slice without extending below layer 6. Neither of these neurons has apical dendritic tufts.

Heavier lines depict dendrites, and thinner lines axons. Laminar boundaries are indicated by horizontal lines. The names of layers are indicated to the left. Note that complete dendritic arbors and descending axons are illustrated, but some axonal arbors are only partially illustrated. Scale bar, 200 μm (A and B).

layer 4Cα, differences in the proportions of cells that received statistically significant input were most apparent when only peak EPSC amplitudes were considered. In this case, cells were discounted if they received significant input from layer 4Cα based on EPSC number or sums of peak amplitudes. Under these conditions, layer 4Cα provided significant excitatory input to 6 of 11 blob cells (55%), 2 of 8 border cells (25%), and 1 of 11 interblob cells (9%; see Table 1). The difference in proportion of blob versus interblob cells was significant (Fisher's exact test, $p = 0.030$). But, as was the case for layer 4B input, when all three EPSC measures were included in the analysis, layer 4Cα input was more uniform with respect to blob location; 8 of 11 blob cells (73%), 4 of 8 border cells (50%), and 5 of 11 interblob cells (45%) received statistically significant input. The differences between populations were again no longer significant.

Layer 4Cm showed a slight bias toward interblob cells (Figure 5A). Our sample of cells with adequate stimulation in 4Cm was small (12 cells) because layer 4Cm is narrow, and only cells with at least ten stimulation sites within a layer were considered for determination of input from that layer (see Experimental Procedures). Nevertheless, 3 of 6 interblob neurons received statistically significant input from 4Cm, while 0 of 2 blob cells or 4 border cells received similar input. Although the difference was not statistically significant (Fisher's exact test, interblob cells versus blob plus border cells, $p = 0.09$), these results are consistent with the observation that a subpopulation of spiny stellate neurons located at the bottom of layer 4Cα or 4Cm has axons that arborize preferentially in interblobs (Yabuta and Callaway, 1998b).

Differences in input for blob versus interblob cells were also detected from layer 5. When considering statistically significant input only in terms of number or sums of EPSC peak amplitudes (excluding cells that had

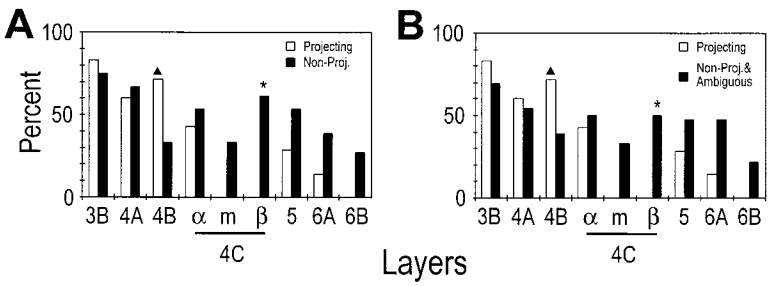

Figure 4. Comparisons of the Layers Providing Input to Projecting versus Nonprojecting Pyramidal Neurons

The histograms illustrate the percentages of layer 3B pyramidal neurons, of different projection types, that received significant input based on EPSC number, peak amplitude, or sums of peak amplitudes from each of the cortical layers.

(A) Percentages for projecting pyramids (open bars) versus local pyramids ("Non-Proj.," closed bars). Asterisk indicates a significant difference between the populations. In this case, 0 of 7 projecting pyramids versus 8 of 13 local pyramids (62%) received significant input from layer 4Cβ (Fisher's exact test, $p = 0.010$). The triangle indicates a significant difference between the populations based on the proportions of cells with significantly larger EPSC amplitudes following stimulation in layer 4B versus control trials. Based on EPSC amplitudes, 5 of 7 (71%) projecting pyramids receive significant layer 4B input versus only 1 of 12 (8%) local pyramids (Fisher's exact test, $p = 0.009$). These proportions are not illustrated in the figure.

(B) Percentages for projecting pyramids (open bars) versus nonprojecting, local pyramids plus neurons with a main descending axon that left the plane of the brain slice ("ambiguous" pyramids, closed bars). Asterisk indicates that the difference in the percentage of cells is significant ($p < 0.05$). Layer 4Cβ input remains significantly less common for projecting pyramids, even with the addition of the ambiguous cells to the local pyramids (0 of 7 versus 10 of 20, Fisher's exact test, $p = 0.022$). The triangle indicates a statistically significant difference between populations when significant input is based on individual EPSC amplitudes. Under these conditions (not illustrated), layer 4B exhibits a statistically significant preference for projecting neurons (5 of 7) versus local plus ambiguous pyramids (3 of 18, $p = 0.016$).

differences based solely on amplitude), layer 5 showed a bias toward blob cells (Figure 5B). For blob cells, 5 of 10 received statistically significant input from layer 5, as opposed to only 1 of 11 interblob cells. This difference was statistically significant (Fisher's exact test, $p = 0.051$), and 3 of 8 border cells also received significant input from this layer. If blob and border cells were pooled together and compared with interblob neurons, the difference remained significant ($p = 0.048$).

Diversity of Input to Individual Neurons

Although there was some specificity of excitatory input to populations of cells based on either morphology or the location of cells with respect to CO blobs, individual neurons received very diverse patterns of laminar input, even within a given population. Close inspection of the laminar sources of input to each of the neurons, as shown in Table 1, reveals that out of the entire population, no 2 cells of the same type (e.g. tufted, nontufted,

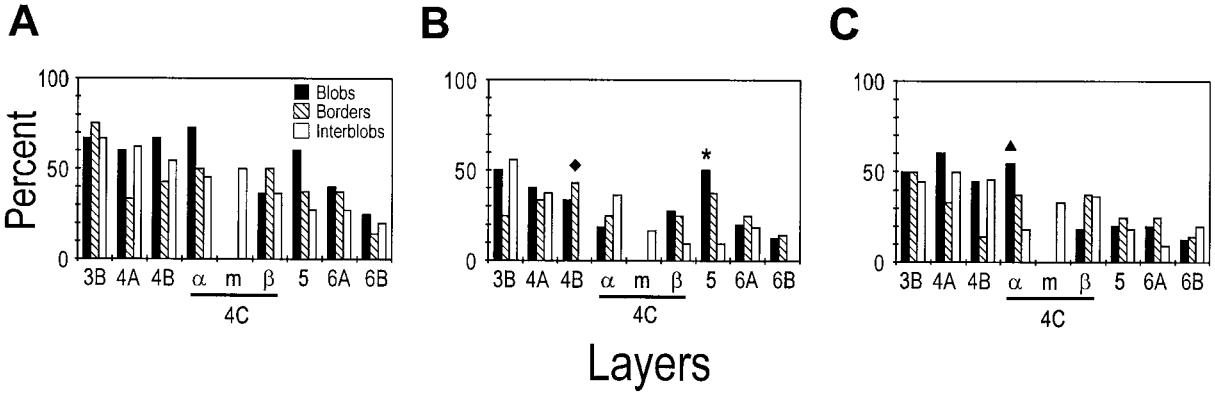

Figure 5. Comparisons of the Layers Providing Input to Neurons in Blobs versus Interblobs

The histograms illustrate the percentages of layer 3B neurons, located in blobs (closed bars), interblobs (open bars), or at blob borders (hatched bars), that received significant input from each of the cortical layers. The EPSC parameters that were used to determine significance of laminar input vary for the different panels (A–C).

(A) Percentages of cells within each group that received significant input based on EPSC number, individual peak amplitudes, or sums of peak amplitudes. Under these analysis conditions, no significant differences between groups or combinations of groups (i.e., blobs plus borders versus interblobs) were detected.

(B) Percentages of cells within each group that received significant input in terms of EPSC number. Cells receiving significant input based only on individual EPSC amplitudes or sums of amplitudes were excluded. Under these conditions, both layers 4B and 5 had a significant preference for blobs and borders. The diamond above layer 4B indicates that when blob and borders cells were pooled together, there was a higher proportion with layer 4B input (6 of 16 cells) than for interblob cells (0 of 11 cells, $p = 0.027$). Asterisk indicates that layer 5 showed a statistically significant preference for cells in blobs (5 of 10 cells) versus interblobs (1 of 11 cells, $p = 0.051$). The difference is also significant if blob and border cells are pooled and compared with interblob cells (8 of 18 versus 1 of 11, $p = 0.048$).

(C) Percentages of cells within each group that received significant input based on individual EPSC peak amplitudes. Cells that received input based on number of EPSCs or sums of amplitudes but not individual amplitudes were excluded. Under these conditions, there were no significant differences between groups or combinations of groups ($p < 0.05$). However, if the comparisons were restricted to cells that received input based solely on individual EPSC amplitudes, excluding any cells with significant input based on EPSC number or sums of amplitudes, then there was preferential input from layer 4Cα to blob versus interblob cells (6 of 11 blob cells versus 1 of 11 interblob cells, $p = 0.030$).

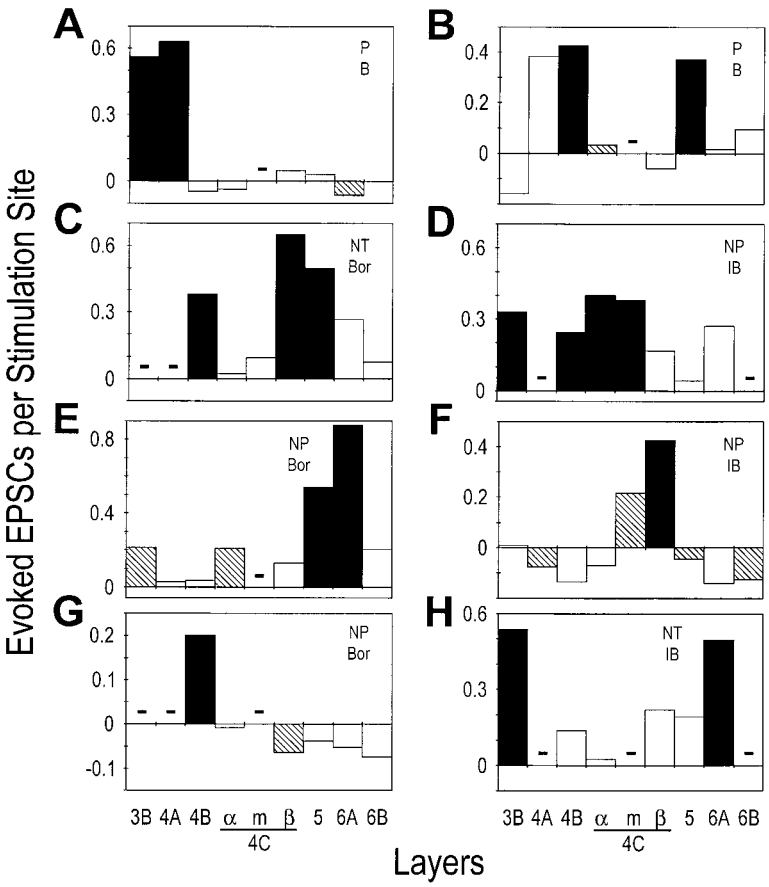

Figure 6. Diversity of Laminar Input to Individual Neurons

The histograms illustrate the mean number of evoked EPSCs (measured minus spontaneous) per stimulation site, from each cortical layer, for 8 layer 3B pyramidal neurons (A–H). Significance of differences in EPSCs measured after photostimulation (versus controls, sEPSCs) for each layer from each cell are indicated by the fill patterns of the corresponding bars. Closed bars indicate a difference (Mann-Whitney U test, $p < 0.05$) based on EPSC number (except for [D], see below). Hatched bars indicate a significant difference based on amplitudes of individual EPSCs but not EPSC number or sums of amplitudes. Open bars indicate no statistical significance. (For the cell shown in [D], the bars for layers 3B and 4B are closed but had significance based on sums of EPSC amplitudes and not EPSC number.) The cell types and locations relative to blobs are indicated by letters at the top right of each histogram. Abbreviations: P, projecting pyramid; NP, nonprojecting, local pyramid; NT, nontufted, ambiguous pyramid; B, blob; IB, interblob; and Bor, blob border. Dash indicates that a value is not shown because there were less than ten stimulation trials in that layer for that cell. (A) through (H) correspond to cells represented in Table 1 as follows: (A) = a40c3, (B) = b38c2, (C) = b38c12, (D) = b35c2, (E) = a40c17, (F) = b34c6, (G) = b38c4, and (H) = b37c14.

or inhibitory) received statistically significant input from the same combination of layers. Thus, the patterns of input to each cell, along with morphological distinctions, reveal that every cell in the sample is a different type. This observation suggests that there are at least 30 cell types in layer 3B (the single neuron of unidentified type, b37c3, is eliminated from this analysis). But, the complete lack of redundancy in our sample implies that there are probably far more types (see Discussion).

The diversity of input is further illustrated in Figure 6, which shows histograms representing the estimated evoked number of EPSCs per stimulation site from each layer for 8 selected pyramidal cells. From the standpoint of either the number of evoked EPSCs for each layer or the patterns of layers that provide statistically significant input, there was considerable heterogeneity in the sources of input to individual neurons. For example, based on the number of EPSCs, the cell depicted in Figure 6E received input from deep layers, 5, and 6A, while the cell in Figure 6G received input from only layer 4B. Both cells were local pyramids located at CO blob borders. However, they had different sources of laminar excitatory input.

There was also little consistency in the number of layers from which individual cells received statistically significant input. For example, the cell depicted in Figure 6F received excitatory input in terms of number of EPSCs from only 1 layer, 4Cβ, while the cell shown in Figure 6D received statistically significant input from all of the superficial layers. Another neuron (cell b31c5; Table 1) received input from all cortical layers that were adequately sampled.

Discussion

We have used scanning laser photostimulation to study the sources of local excitatory connections to individual layer 3B neurons in the primary visual cortex of macaque monkeys. We found both greater specificity and greater diversity of connections to individual neurons than could be inferred from anatomical observations. For example, anatomical observations reveal a dense projection from layer 4Cβ spiny stellate neurons to layer 3B (cf. Yabuta and Callaway, 1998b). However, photostimulation reveals excitatory input only onto layer 3B local pyramids (pyramidal neurons whose axonal arbors are local to V1). No layer 4Cβ input is detected onto layer 3B projecting pyramids. Thus, despite extensive overlap of the axonal arbors of layer 4Cβ spiny stellate neurons with the dendritic arbors of both projecting and local pyramids, functional connections are preferentially made onto local pyramids. The observation that differences in functional input can be correlated with differences in dendritic morphology suggests that in future studies it will be possible to correlate morphological features with differences in visual responses in vivo, providing a link between differences in functional input and visual receptive fields.

Although different cell types can receive input from different sources, there is still further specificity of local connections. Even neurons with similar morphological

features or at similar locations relative to CO blobs receive highly diverse laminar sources of local input. Within our population of 31 neurons, no 2 cells of the same morphological type received significant input from the same combination of layers. Thus, based on connectional distinctions, there are far more cell types than expected based on morphological features alone.

These observations have important implications for understanding general principles of the organization and function of cortical connections. For example, the number of cell types in a cortical area has important implications for the amount of redundancy that is required to compensate for uncertainty in the representations encoded by individual neurons (cf. Stevens, 1998). Also, along with comparisons of the sources of input to layer 3B blob versus interblob neurons, these results provide insight into the neural mechanisms that underlie visual processing in macaque V1.

Another important implication of our findings is that overlap of axonal arbors with dendritic arbors does not imply that functional connections must exist between the 2 cell types. Thus, individual cells within a single layer or with overlapping dendritic arbors can play distinct roles in cortical function. Furthermore, similarities in the anatomical organization of circuits between cortical areas or between analogous areas from different species do not imply that the organization of functional connections must also be similar. Until a more general understanding of any possible rules of cortical connectivity becomes available, the precise connectivity of neurons in one cortical area cannot be inferred from observations in another.

Diversity of Input to Individual Neurons

Despite overall trends in the laminar sources of excitatory input according to cell type or location relative to blobs, individual layer 3B neurons that were categorized as members of the same population invariably received functional input from different layers. This diversity suggests that embedded within the laminar and columnar cortical organization defined by CO staining, there exists a finer level of organization not detectable by the anatomy.

The diversity of functional input to individual neurons has important implications for understanding how populations of cortical neurons represent information about the environment and the extent to which neuronal redundancy is utilized to compensate for variability in neuronal responses or neuron death (Stevens, 1998). Stevens (1998) calculates that there are a sufficient number of neurons in typical primate cortex (not V1) such that each type could tile the cortex even if there were 5000 types (this is the number of unique cell types predicted if there is no functional redundancy). We have used the cell densities described for each layer in monkey V1 (Beaulieu et al., 1992) to make a similar calculation for layer 3B. We estimate that tiling could be achieved in layer 3B even if there were as many as 1000 different neuron types in this layer.

To estimate the functional redundancy in layer 3B, we next need to estimate the number of connectionally distinct cell types. For example, if there are 100 cell types in layer 3B, then there is 10-fold (1000/100 = 10) functional redundancy. If we take at face value the observation that 0 of 30 neurons in our sample received excitatory input from the same combination of layers, then there are at least 30 cell types, and probably far more. But how many more? One can estimate a lower limit on the number of cell types if it is assumed that all cell types are equally represented (if this assumption were incorrect, then the number of cell types would be greater than calculated below). Then the probability, p, of obtaining a sample of size n with no 2 cells alike is $p = N!/N^n(N\text{-}n)!$, where N is the number of cell types. If we place our confidence level at $p = 0.05$, then with our sample of $n = 30$ cells, $N = 156$ cell types. Thus, 19 of 20 times, one would expect that at least 2 cells in a sample of 30 would be the same type, even if there were as many as 156 types. Our data are therefore suggestive of at least 156 cell types in layer 3B, consistent with the 511 possible combinations of input from 9 different layers ($2^9 - 1 = 511$).

The data should, however, be interpreted with some caution. If we fail to detect statistically significant input above spontaneous activity levels for a particular layer, it cannot be concluded with certainty that there was no input from that layer. The number of stimulation sites might have been too small to detect weak input, or input may have been cut during brain slice preparation. For example, since the generation of action potentials by photostimulation is restricted to neurons near the edge of the slice (see Experimental Procedures), the axons of stimulated cells in deep layers could leave the slice before reaching layer 3B. This effect is minimized, however, because axons projecting to superficial layers rise vertically from deep layer cell bodies (Callaway and Wiser, 1996; Wiser and Callaway, 1996; Yabuta and Callaway, 1998b). Thus, it is possible that in some cases, 2 cells receiving input from the same combination of layers were counted as different because of undetected input. Nevertheless, even in the face of these considerations, there appear to be a large number of connectionally distinct cell types in layer 3B. The 156 types estimated quantitatively is the minimum number suggested by the data. Thus, it is reasonable to infer that there are probably at least 100 cell types and therefore not more than 10-fold functional redundancy. Even if there were only 50 cell types, there would still be just 20-fold redundancy. Together, these observations and inferences argue that unique information is carried by just a handful of neurons, on the order of ten, not hundreds or thousands, as might be inferred from the limited anatomical diversity of cortical neurons.

Implications for Visual Processing

The organization of visual cortical circuits has both parallel and hierarchical features. This organization applies to both connections between cortical areas (see Felleman and Van Essen, 1991) and local connections within V1 (see Callaway, 1998). Our studies of local input to layer 3B neurons have implications for both of these aspects of V1 local circuits.

V1 lies at the bottom of a hierarchy of cortical areas, as it receives the great majority of direct input relayed to the visual cortex from the retina via the dLGN (Benevento and Standage, 1982; Bullier and Kennedy, 1983).

The retino–geniculo–cortical pathway is separated into parallel pathways, including the M (magnocellular) and P (parvocellular) pathways (see Livingstone and Hubel, 1988; Merigan and Maunsell, 1993; Casagrande, 1994, for reviews). "Higher" extrastriate cortical areas, which receive their input either directly or indirectly from V1, are also organized into separate streams (see Desimone and Ungerleider, 1989). The dorsal stream includes visual areas involved in determining spatial relationships between objects. These areas are thought to be closely associated with the fast but color-blind M pathway and receive their input directly and indirectly from layer 4B of V1. The ventral stream areas are involved in object identification, receive input via layer 2/3 of V1, and are thought to be more closely associated with the chromatically sensitive and high–spatial resolution P pathway. But, both anatomical and physiological studies reveal that there is likely to be considerable interaction between M and P pathways mediated by local circuits within V1, such that both pathways make some contributions to both dorsal and ventral streams (see Merigan and Maunsell, 1993; Callaway, 1998, for reviews).

Hierarchical Local Circuits

Anatomical studies of V1 circuits reveal a local hierarchical organization in which layer 4C receives direct dLGN input, which is relayed to more superficial layers, and then out to higher extrastriate cortical areas (see Callaway, 1998). Within the M pathway, only a single synapse separates dLGN recipient neurons in layer 4Cα from neurons in layer 4B that project to dorsal visual areas. This fast transmission of visual information to dorsal cortical areas, particularly the middle temporal area (MT), is consistent with the prominent role of these areas in the analysis of motion (Merigan and Maunsell, 1993). Lachica et al. (1992) suggested a more complex hierarchical relationship within layer 2/3 of macaque V1. Since layer 4C neurons have axonal arbors in layer 3B but not layer 2/3A (see also Callaway and Wiser, 1996; Yabuta and Callaway, 1998b), and most projections from layer 2/3 to extrastriate cortex come from layer 2/3A (Rockland and Pandya, 1979; Yukie and Iwai, 1985; Callaway and Wiser, 1996), there is a multisynaptic pathway involving projections from layer 4C to 3B and then to layer 2/3A projection neurons. But, these anatomical observations do not resolve the issue of whether a multisynaptic pathway is obligatory. Layer 3B projection neurons could provide a more direct path to ventral visual areas. The actual path depends on whether the minority, projecting pyramids in layer 3B, receive direct connections from layer 4C.

With photostimulation, we have detected direct input from layer 4Cα onto layer 3B projection neurons but not from layer 4Cβ—the 4Cβ connections are specific for local pyramids. Thus, the "extra synapse" appears to be an obligatory step for the P pathway, but the M pathway takes the more direct path. The faster transmission of information from the M stream therefore applies not only to information sent to dorsal stream visual areas via layer 4B but also to information sent to ventral stream areas via layer 3B. The P pathway to ventral areas appears to be slower, not only due to slower conduction velocities (Bullier and Nowak, 1995) but also to more extensive processing within area V1.

Parallel Local Circuits

V1 is where the M and P pathways first give rise to the dorsal and ventral streams, with layer 4B providing input to dorsal areas and layer 2/3 to ventral areas (see Felleman and Van Essen, 1991). In addition, the main recipient of input from layer 2/3, area V2, is separated into functionally discrete regions that stain differentially for CO and receive input from V1 blobs (V2 thin CO stripes) versus interblobs (V2 pale stripes) (Livingstone and Hubel, 1983; DeYoe and Van Essen, 1985; Hubel and Livingstone, 1987; Levitt et al., 1994). The V2 thin and pale stripes in turn project to functionally and anatomically distinct subdivisions of still higher visual areas (Shipp and Zeki, 1985, 1995; Zeki and Shipp, 1989; DeYoe et al., 1994). Anatomical observations suggest specific relationships between the M and P pathways and the CO blob and interblob regions of layer 2/3 (Lachica et al., 1992; Yoshioka et al., 1994; Yabuta and Callaway, 1998b; see Callaway, 1998, for review). Blob regions preferentially receive axonal projections from the M pathway recipient layer 4Cα and from layer 4B. Interblob regions, in contrast, are preferentially targeted by afferents from a subpopulation of highly stratified spiny stellate cells located in layer 4Cm (lower 4Cα). P recipient spiny stellate neurons in layer 4Cβ project densely to both blobs and interblobs.

These anatomical observations do not, however, reveal functional connectivity with the level of specificity afforded by photostimulation. For example, we observe that individual neurons often receive connections preferentially from a subset of the layers containing neurons with axonal projections overlapping spatially with their dendrites. Thus, connections can be more specific than predicted from anatomical observations. On the other hand, the dendritic arbors of layer 2/3 neurons can freely cross between blob and interblob regions (Hubener and Bolz, 1992; Malach, 1992), providing access to inputs whose axons do not arborize at the location of the cell body.

Our photostimulation experiments revealed connections that are, on the whole, consistent with the anatomical observations. Preferential connections to blobs were observed from both layers 4Cα and 4B. However, these preferences were not as strong as expected; photostimulation revealed significant input to cells in both blobs and interblobs. Differences in the proportion of blob versus interblob cells receiving significant input from these layers depended on what parameters of the EPSCs were evaluated. In addition, we observed an unexpected preference for blobs following stimulation in layer 5.

Experimental Procedures

Slice Preparation

Macaque V1 brain slices were prepared using methods described in detail previously (Callaway and Wiser, 1996; Wiser and Callaway, 1996). The methods used here sometimes differed from previously described reports in that during surgery to collect cortical tissue, inhaled isoflurane (1%–3% in O_2) was sometimes used instead of sodium pentobarbitol to maintain anesthesia following an initial dose of ketamine (10–20 mg/kg i.m.). In addition, in some cases, a portion of V1 was removed from one hemisphere for preparation of brain slices during a recovery surgery. This was followed by a nonrecovery

surgery 5–10 days later to harvest tissue from the remaining intact hemisphere.

Data described here were collected from nine macaque monkeys, with age, sex, species, and number of cells sampled per animal as follows: (1) B31, 11 months, male, *M. mulatta*, 1 cell; (2) B32, 13.5 months, male, *M. mulatta*, 2 cells; (3) B33, 15 months, male, *M. mulatta*, 2 cells; (4) B34, 18 months, female, *M. radiata*, 2 cells; (5) B35, 17 months, male, *M. mulatta*, 3 cells; (6) B36, 17 months, male, *M. mulatta*, 4 cells; (7) B37, 17 months, male, *M. mulatta*, 5 cells; (8) B38, 14 months, male, *M. mulatta*, 6 cells; and (9) A40, 14 months, male, *M. mulatta*, 6 cells. Specific cells are identified by the parent animal in Table 1.

Photostimulation and Whole-Cell Recording

Individual brain slices were transferred to a recording chamber, where they were submerged in recirculating, oxygenated (95% O_2, 5% CO_2) artifical cerebrospinal fluid (ACSF) containing 150 μM CNB caged glutamate (L-glutamic acid γ-(α-carboxy-2-nitro-benzyl) ester, trifluoroacetic acid salt; Molecular Probes) at room temperature. Whole-cell recordings monitoring synaptic responses were obtained from individual layer 3B neurons within the slice (Blanton et al., 1989). Glass electrodes (5–15 MΩ) were filled with a standard intracellular solution (130 mM potassium gluconate, 1 mM EGTA, 2 mM $MgCl_2$, 0.5 mM $CaCl_2$, 2.54 mM ATP, and 10 mM HEPES [pH = 7.3]) containing 0.5% biocytin. Recorded neurons were held in voltage clamp to a membrane potential of -65 mV. Only excitatory inward synaptic currents evoked by the stimulation paradigm were considered.

Photostimulation was accomplished by uncaging the glutamate with a shutter-controlled 10 ms flash of continuous beam ultraviolet (UV) argon ion laser light ($\sim$25 mW at the specimen). The light was focused through a coverslip beneath the slice to a diffraction-limited spot within the slice using a 40$\times$ oil immersion microscope objective (Nikon Fluor 40$\times$, 1.4NA). The concentration of caged glutamate and duration and intensity of UV light flashes were selected because control experiments revealed that under these conditions, only neurons with their cell bodies very near the flash site generated APs (see details below). Thus, if EPSCs are evoked, it can be inferred that neurons with cell bodies near the stimulation site have functional, monosynaptic connections onto the recorded cell.

Since this study focused on the interlaminar connectivity of individual layer 3B neurons, vertical columns normal to the layers were stimulated in a pseudorandom pattern. The light flash location was moved by mounting the optics on a computer controlled X–Y translation stage (Dalva and Katz, 1994; Katz and Dalva, 1994; Sawatari and Callaway, 1996). Within each slice, 100–500 sites were stimulated. The stimulation sequences assured that sites separated by $<$200 μm were always stimulated more than 10 s apart. This assured that stimulation at a given site was not influenced by the desensitization of glutamate receptors following uncaging at a previous site.

For 20 ms preceding and 380 ms following photostimulation at each site, the output from the whole-cell recording amplifier was digitized at 10 kHz and stored to allow later analysis of EPSCs (see below). Motor encoder counts indicating the X–Y coordinates of the stimulation site were also stored in association with the corresponding electrical recording. Stimulation trials were regularly interspersed with control, no-stimulation (shutter closed) trials to allow later analysis of sEPSCs and to monitor possible changes in access resistance of electrical recordings. During the control trials, 400 ms of amplifier output was digitized with a 35 ms duration $+10$ mV voltage step introduced at 300 ms. The first 300 ms of the recording was used to assay sEPSCs, and the response to the voltage step to monitor access resistance. Spontaneous currents were later compared with responses to photostimulation in order to determine whether EPSCs were stimulus dependent or noise (see below).

Histology and Anatomical Analysis

After completion of photostimulation, fiducial marks were made within the slice to allow the alignment of anatomical locations with stimulation sites. Alignment sites were made using 3 s duration flashes of UV laser light onto the cortical tissue, which resulted in the bleaching of CO staining in the exposed area. The motor encoder counts corresponding to the alignment site locations were saved to allow later alignment of the anatomical and physiological coordinate systems.

Slices were then fixed, resectioned, and double stained for CO and biocytin as described previously (Callaway and Wiser, 1996; Wiser and Callaway, 1996). After staining, camera lucida drawings were made, including the axonal and dendritic arbors of labeled neurons, laminar boundaries, CO blobs, and alignment sites. Sections were then counterstained with thionin to confirm laminar borders and to distinguish the 4Cα/4Cβ and 6A/6B borders, which are not discernible with CO stain alone (see Yabuta and Callaway, 1998b). We defined the middle of layer 4C, 4Cm, as the bottom fifth of layer 4Cα because the neurons here have different patterns of axonal arbors than those in the upper four-fifths of 4Cα, which we refer to as 4Cα (Yabuta and Callaway, 1998b). The anatomical data were then scanned into a computer and saved as a graphics file. Alignment sites were used to align the anatomical reconstruction with the location of photostimulation sites. Custom software was then used to translate anatomical features into the coordinate space of the photostimulation data. Each stimulation site was then assigned to the correct layer.

Analysis of EPSCs and Layer-Specific Input Patterns

For each recorded neuron, the numbers and peak amplitudes of EPSCs generated within 150 ms following the laser flash for each stimulation site were determined using custom software. EPSCs in each 150 ms record were first picked by passing traces through a postsynaptic current discrimination program (comparing a template generated by averaging 50 EPSCs with individual traces using a least-squares fit algorithm). The traces were then rechecked manually to minimize potential errors made by the discriminator. Windows of control (150 ms; no stimulation) traces were analyzed using identical procedures.

After recordings for a particular cell were analyzed, the significance of the occurrence and size of EPSCs measured following stimulation of a given layer were assessed. This was done by comparing the distributions of the numbers, individual peak amplitudes, or sums of peak amplitudes of EPSCs from each stimulation site in a given layer with the distributions of the same parameters for spontaneous currents (no stimulation controls) from the cell. The Mann-Whitney U test was used to determine the significance of each of these measures of EPSCs following photostimulation relative to sEPSCs. To estimate the relative input from each layer to a given cell, histograms were generated depicting the estimated mean number of evoked EPSCs per stimulation site (estimated mean evoked = mean photostimulation $-$ mean spontaneous) obtained for each layer (e.g., Figure 6).

Analysis of Groups of Neurons

To determine if there were systematic differences in the patterns of excitatory laminar input to different cell types or cells in different blob/interblob regions, each neuron was categorized in terms of (1) cell type, i.e., pyramidal or inhibitory; (2) whether the axons of pyramidal neurons projected to the white matter; (3) whether pyramidal neurons had apical dendritic tufts; and (4) where the neuron's cell body was located with respect to CO blobs. Cells were then counted within each group in terms of whether they had or had not received significant input from a given layer. This procedure was repeated for all layers. Only layers that had at least ten stimulation sites were included in the tally. The significance of differences in the proportion of cells that received excitatory input from a given layer between groups was determined by conducting Fisher exact tests. This was repeated for all layers.

Spatial Resolution of Photostimulation

Photostimulation-evoked EPSCs must result from the generation of APs in a neuron making a monosynaptic connection to the recorded cell. Thus, the spatial resolution of the photostimulation method is determined by the distance from a neuron's cell body over which the UV light flash can evoke APs. Since cells far from the stimulation site never fire APs (see below), it can be inferred that the detection of stimulus-evoked EPSCs indicates the presence of a monosynaptic connection from 1 or more cells at the stimulation site onto the recorded neuron. Polysynaptic activation of EPSCs via cells farther

from the stimulation site would require that the intermediary cells fire action potentials. The control experiments below demonstrate that with the stimulus parameters used, APs are not detected in neurons with cell bodies far from the stimulation site.

The spatial resolution of the photostimulation method was assessed by measuring the distance over which APs could be generated in cells recorded intracellularly in current-clamp mode when directly photostimulating with the laser light. Using the blind patching configuration, with photostimulation from below the slice and recording from above, APs were never generated in recorded neurons. This is presumably because the UV light coming from below was scattered by the brain tissue, preventing focal uncaging near the cell body. We therefore used a visualized patching rig to measure direct activation of neurons with cell bodies located within the focal plane. A 40× water immersion objective (Olympus LUMPlanFl 40×, 0.8NA) was used to focus the light through the ACSF from above the slice. The laser was adjusted such that the UV light at the specimen was the same intensity as for the blind patching experiments. The focus was adjusted to the depth of the recorded neuron's cell body, which was visualized with infrared differential interference contrast optics to obtain the whole-cell recording.

Using the same light parameters and glutamate concentrations as for the mapping experiments, cells targeted with the visualized patch rig were stimulated directly while held in current clamp. In monkey V1, 15 cells were tested in this manner. Of these, 10 generated APs as a result of the uncaging: 6 layer 4Cα cells, 1 layer 4B cell, 2 layer 3B cells, and 1 layer 6 cell. The other 5 cells were depolarized by photostimulation, but regardless of the position of the light flash, they could not be depolarized above threshold for AP generation.

For the 10 neurons with APs, the mean distance over which at least one AP was generated was 71.8 μm (horizontal) × 126.5 μm (vertical). The mean values by layer were 56.5 × 124.4 μm (horizontal/vertical) for 4Cα, 141.2 × 84.7 μm for 4B, 22.1 × 98.5 μm for 3B, and 193.5 × 237.1 μm for layer 6. The largest responses were invariably centered at the cell body, so these values translate into a 35.9 × 63.3 μm "radius" of AP generation from the cell body center. These values reduced to 35.4 × 43.3 μm when only those sites that resulted in the generation of two or more APs were considered.

Acknowledgments

We thank Jami Dantzker and Drs. Emily Huang and John Wesseling for providing and helping to develop software for data analysis. We also thank Jami Dantzker for helpful discussions and for her contribution to technical improvements in photostimulation methods. We thank Dr. Charles Stevens for helpful discussions and comments on the manuscript and for deriving the equation to estimate the number of unique cell types in a population. This work was supported by National Institutes of Health grant EY10742 (E. M. C.). A. S. was supported by a National Institutes of Health training grant (GM08107), the Chapman Charitable Trust, the Salk Institute Association, and the Timken-Sturgis Foundation.

Received July 26, 1999; revised December 9, 1999.

References

Anderson, J.C., Martin, K.A.C., and Whitteridge, D. (1993). Form, function, and intracortical projections of neurons in the striate cortex of the monkey *Macacus nemestrinus*. Cereb. Cortex *3*, 412–420.

Beaulieu, C., Kisvardy, Z., Somogyi, P., Cynader, M., and Cowey, A. (1992). Quantitative distribution of GABA-immunopositive and -immunonegative neurons and synapses in the monkey striate cortex (Area 17). Cereb. Cortex *2*, 295–309.

Benevento, L.A., and Standage, G.P. (1982). Demonstration of lack of dorsal lateral geniculate nucleus input to extrastriate areas MT and visual 2 in the macaque monkey. Brain Res. *252*, 161–166.

Blanton, M.G., Lo Turco, J.J., and Kriegstein, A.R. (1989). Whole cell recording from neurons in slices of reptilian and mammalian cerebral cortex. J. Neurosci. Methods *30*, 203–210.

Bullier, J., and Kennedy, H. (1983). Projection of the lateral geniculate nucleus onto cortical area V2 in the macaque monkey. Exp. Brain Res. *53*, 168–172.

Bullier, J., and Nowak, L.G. (1995). Parallel versus serial processing: new vistas on the distributed organization of the visual system. Curr. Opin. Neurobiol. *5*, 497–503.

Callaway, E.M. (1998). Local circuits in primary visual cortex of the macaque monkey. Annu. Rev. Neurosci. *21*, 47–74.

Callaway, E.M., and Katz, L.C. (1993). Photostimulation using caged glutamate reveals functional circuitry in living brain slices. Proc. Natl. Acad. Sci. USA *90*, 7661–7665.

Callaway, E.M., and Wiser, A.K. (1996). Contributions of individual layer 2-5 spiny neurons to local circuits in macaque primary visual cortex. Vis. Neurosci. *13*, 907–922.

Casagrande, V.A. (1994). A third parallel visual pathway to primate area V1. Trends Neurosci. *17*, 305–310.

Dalva, M.B., and Katz, L.C. (1994). Rearrangements of synaptic connections in visual cortex revealed by laser photostimulation. Science *265*, 255–258.

Desimone, R., and Ungerleider, L. (1989). Neural mechanisms of visual processing in monkeys. In Handbook of Neuropsychology, F. Boller and J. Grafman, eds. (New York: Elsevier), pp. 267–299.

DeYoe, E.A., and Van Essen, D.C. (1985). Segregation of efferent connections and receptive field properties in visual area V2 of the macaque. Nature *317*, 58–61.

DeYoe, E.A., Felleman, D.J., Van Essen, D.C., and McClendon, E. (1994). Multiple processing streams in occipitotemporal visual cortex. Nature *371*, 151–154.

Edwards, D.P., Purpura, K.P., and Kaplan, E. (1995). Contrast sensitivity and spatial frequency response of primate cortical neurons in and around the cytochrome oxidase blobs. Vision Res. *35*, 1501–1523.

Felleman, D.J., and Van Essen, D.C. (1991). Distributed hierarchical processing in the primate cerebral cortex. Cereb. Cortex *1*, 1–47.

Hubel, D.H., and Livingstone, M.S. (1987). Segregation of form, color, and stereopsis in primate area 18. J. Neurosci. *7*, 3378–3415.

Hubel, D.H., and Wiesel, T.N. (1968). Receptive fields and functional architecture of monkey striate cortex. J. Physiol. *195*, 215–243.

Hubel, D.H., and Wiesel, T.N. (1974). Sequence regularity and geometry of orientation columns in the monkey striate cortex. J. Comp. Neurol. *158*, 267–294.

Hubener, M., and Bolz, J. (1992). Relationships between dendritic morphology and cytochrome oxidase compartments in monkey striate cortex. J. Comp. Neurol. *324*, 67–80.

Katz, L.C., and Dalva, M.B. (1994). Scanning laser photostimulation: a new approach for analyzing brain circuits. J. Neurosci. Methods *54*, 205–218.

Katz, L.C., Gilbert, C.D., and Wiesel, T.N. (1989). Local circuits and ocular dominance columns in monkey striate cortex. J. Neurosci. *9*, 1389–1399.

Lachica, E.A., Beck, P.D., and Casagrande, V.A. (1992). Parallel pathways in macaque monkey striate cortex: anatomically defined columns in layer III. Proc. Natl. Acad. Sci. USA *89*, 3566–3570.

Levitt, J.B., Kiper, D.C., and Movshon, J.A. (1994). Receptive fields and functional architecture of macaque V2. J. Neurophysiol. *71*, 2517–2542.

Livingstone, M., and Hubel, D. (1988). Segregation of form, color, movement, and depth: anatomy, physiology, and perception. Science *240*, 740–749.

Livingstone, M.S., and Hubel, D.H. (1983). Specificity of cortico–cortical connections in monkey visual system. Nature *304*, 531–534.

Livingstone, M.S., and Hubel, D.H. (1984a). Anatomy and physiology of a color system in the primate visual cortex. J. Neurosci. *4*, 309–356.

Livingstone, M.S., and Hubel, D.H. (1984b). Specificity of intrinsic connections in primate primary visual cortex. J. Neurosci. *4*, 2830–2835.

Lund, J.S. (1987). Local circuit neurons of macaque monkey striate

cortex: I. Neurons of laminae 4C and 5A. J. Comp. Neurol. *257*, 60–92.

Lund, J.S., and Yoshioka, T. (1991). Local circuit neurons of macaque monkey striate cortex: neurons of laminae 4B, 4A, and 3B. J. Comp. Neurol. *311*, 234–258.

Lund, J.S., Hawken, M.J., and Parker, A.J. (1988). Local circuit neurons of macaque monkey striate cortex: II. Neurons of laminae 5B and 6. J. Comp. Neurol. *276*, 1–29.

MacNeil, M.A., and Masland, R.H. (1998). Extreme diversity among amacrine cells: implications for function. Neuron *20*, 971–982.

Malach, R. (1992). Dendritic sampling across processing streams in monkey striate cortex. J. Comp. Neurol. *315*, 303–312.

Merigan, W.H., and Maunsell, J.H.R. (1993). How parallel are the visual pathways? Annu. Rev. Neurosci. *16*, 369–402.

Parra, P., Gulyas, A.I., and Miles, R. (1998). How many subtypes of inhibitory cells in the hippocampus? Neuron *20*, 983–993.

Rockland, K.S., and Pandya, D.N. (1979). Laminar origins and terminations of cortical connections of the occipital lobe in the rhesus monkey. Brain Res. *179*, 3–20.

Sawatari, A., and Callaway, E.M. (1996). Convergence of magno- and parvocellular pathways in layer 4B of macaque primary visual cortex. Nature *380*, 442–446.

Shipp, S., and Zeki, S. (1985). Segregation of pathways leading from area V2 to areas V4 and V5 of macaque monkey visual cortex. Nature *315*, 322–325.

Shipp, S., and Zeki, S. (1995). Segregation and convergence of specialised pathways in macaque monkey visual cortex. J. Anat. *187*, 547–562.

Stevens, C.F. (1998). Neuronal diversity: too many cell types for comfort? Curr. Biol. *8*, R708-R710.

Tootell, R.B., Hamilton, S., Silverman, M.S., and Switkes, E. (1988a). Functional anatomy of macaque striate cortex: I. Ocular dominance, binocular interactions, and baseline conditions. J. Neurosci. *8*, 1500–1530.

Tootell, R.B., Hamilton, S., and Switkes, E. (1988b). Functional anatomy of macaque striate cortex: IV. Contrast and magno–parvo streams. J. Neurosci. *8*, 1594–1609.

Tootell, R.B., Silverman. M.S., Hamilton, S., Switkes, E., and De Valois, R.L. (1988c). Functional anatomy of macaque striate cortex: V. Spatial frequency. J. Neurosci. *8*, 1610–1624.

Ts'o, D.Y., Gilbert, C.D., and Wiesel, T.N. (1986). Relationships between horizontal interactions and functional architecture in cat striate cortex as revealed by cross-correlation analysis. J. Neurosci. *6*, 1160–1170.

Wiser, A.K., and Callaway, E.M. (1996). Contributions of individual layer 6 pyramidal neurons to local circuitry in macaque primary visual cortex. J. Neurosci. *16*, 2724–2739.

Yabuta, N.H., and Callaway, E.M. (1998a). Cytochrome oxidase blobs and intrinsic horizontal connections of layer 2/3 pyramidal neurons in primate V1. Vis. Neurosci. *15*, 1007–1027.

Yabuta, N.H., and Callaway, E.M. (1998b). Functional streams and local connections of layer 4C neurons in primary visual cortex of the macaque monkey. J. Neurosci. *18*, 9489–9499.

Yoshioka, T., Levitt, J.B., and Lund, J.S. (1994). Independence and merger of thalamocortical channels within macaque monkey primary visual cortex: anatomy of interlaminar projections. Vis. Neurosci. *11*, 467–489.

Yukie, M., and Iwai, E. (1985). Laminar origin of direct projection from cortex area V1 to V4 in the rhesus monkey. Brain Res. *346*, 383–386.

Zeki, S., and Shipp, S. (1989). Modular connections between areas V2 and V4 of macaque monkey visual cortex. Eur. J. Neurosci. *1*, 494–506.